A deep look at the HESS J1825-137 pulsar wind nebula with H.E.S.S. and Fermi-LAT

LPNHE PARIS

Sami Caroff, Alison Mitchell, Giacomo Principe, Stefan Funk, Joachim Hahn, Jim Hinton, Daniel Parsons

Based on « Particle Transport within the Pulsar Wind Nebula HESS J1825-137 » (https://arxiv.org/abs/1810.12676) and « Energy dependent analysis of the pulsar wind nebula HESS J1825-137 with Fermi-LAT » (in prep)

The HESS J1825-137 pulsar wind nebulae

- HESS J1825-137 VHE nebula **discovered by H.E.S.S.** in 2005 (extent 0.5°)
- First evidence of its **energy dependent morphology** in 2006 by H.E.S.S.
- **Extended emission region** found in X-rays by ROSAT and ASCA (~4'), XMM-Newton (5'), Chandra and Suzaku (15')
- **Very likely associated** with the **PSR B1823-13** :
  - Age : 2.14×10^4 yr
  - Spin-down power : 2.8×10^{36} erg.s^{-1}
  - Period : 0.1015 s
  - Distance : ~4 kpc
- Nebula found to be **asymmetric** compared to the potential progenitor in both gamma-ray and X-ray (toward South)
- VLA radio observations of PSR B1823-13 → **proper motion** of 443 ± 46 km.s^{-1}, perpendicular to the nebula extent
- EVLA radio observations found a **molecular cloud in the North** (~ 400 cm^{-3})
- **Observed by Fermi-LAT** in 2011, extent of 0.56° ± 0.07°, in the FGES, extent 1.05°±0.25°
- **HAWC detection** of a significant excess coming from the region, but can't disentangle with HESS J1826-130

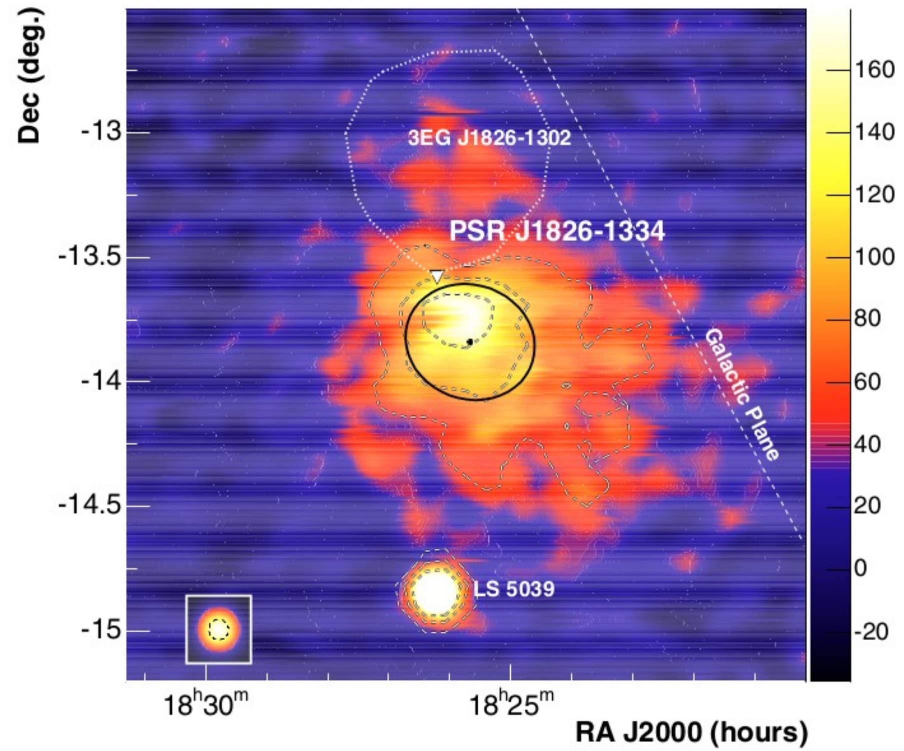

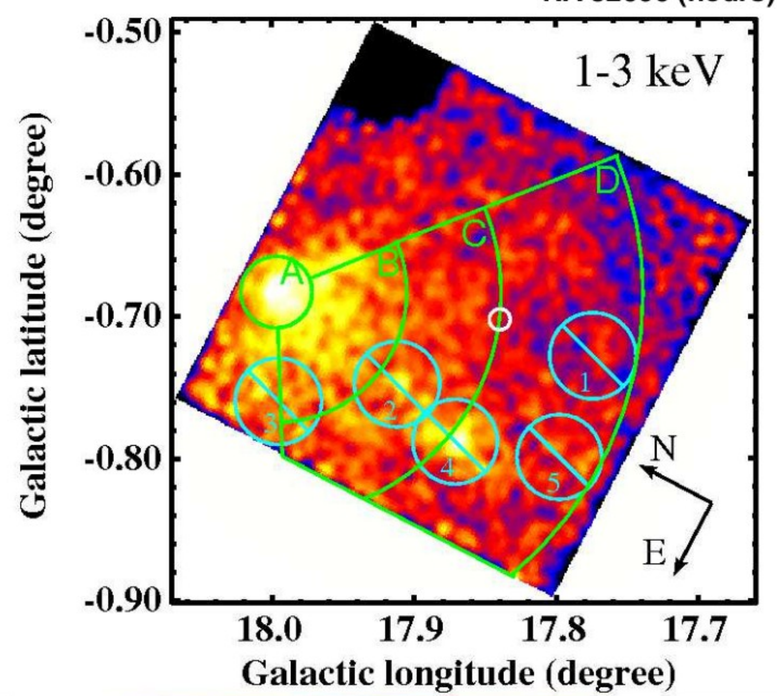

HESS J1825-137 Analysis

Analysis	Telescopes	Exposure	Time Period	θ_z
A	CT1-4	387 hours	2004 - 2016	25.8°
B	CT1-5	136 hours	2012 - 2016	23.2°

Table 1. Summary of the data used in the two analyses, including the exposure and mean zenith angle θ_z of the observations. The data for analysis B were also used in analysis A, but without CT5.

- Very rich dataset,~400h of exposure time
- Two dataset used :
  - A is CT1-4 only telescope used
  - B is CT1-5 (2012-2016)
- Complex region :
  - HESS J1826-130 North
  - LS 5039 South
- Large excess regions, asymmetric geometry compared to PSR B1823-13
- PSF little compared to the angular size of the nebula → permits a deep morphology analysis of the nebula

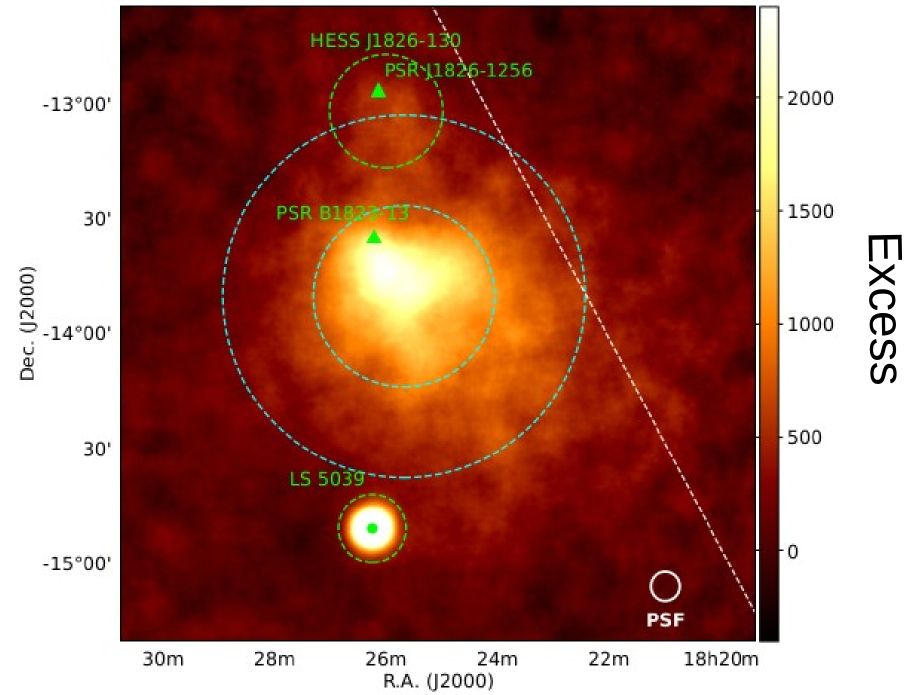

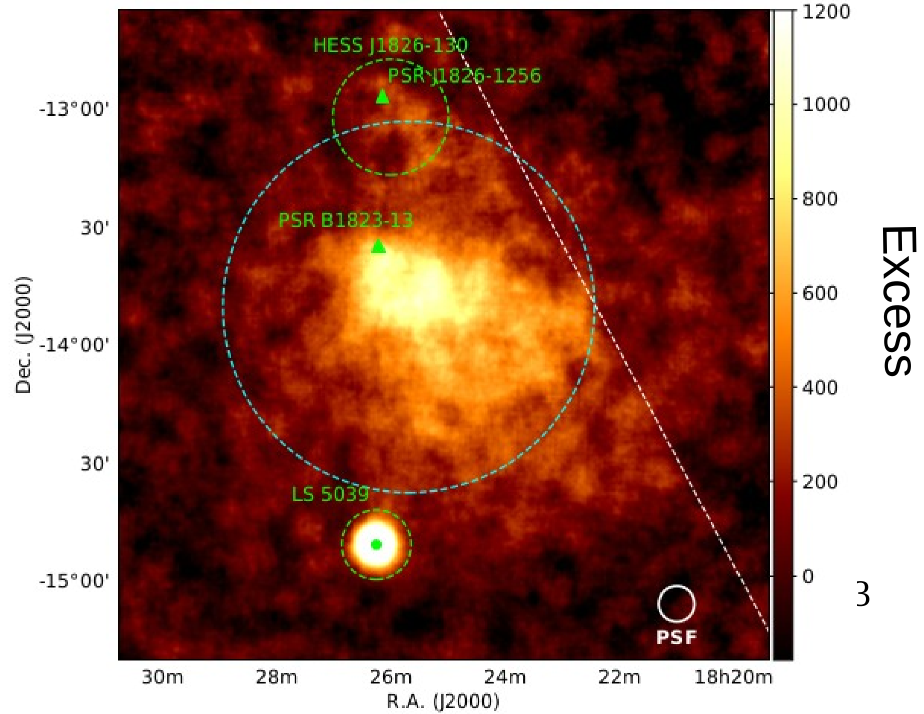

HESS J1825-137 spectral analysis

- Spectral analysis of 0.4° and 0.8° region size
- Significant Flux observed up to ~50 TeV
- HESS J1825-137 dominates its neighbor HESS J1826-130 on the full energy scale
- HAWC excess likely comes from HESS J1825-137
- Cut-off observed at 19 TeV

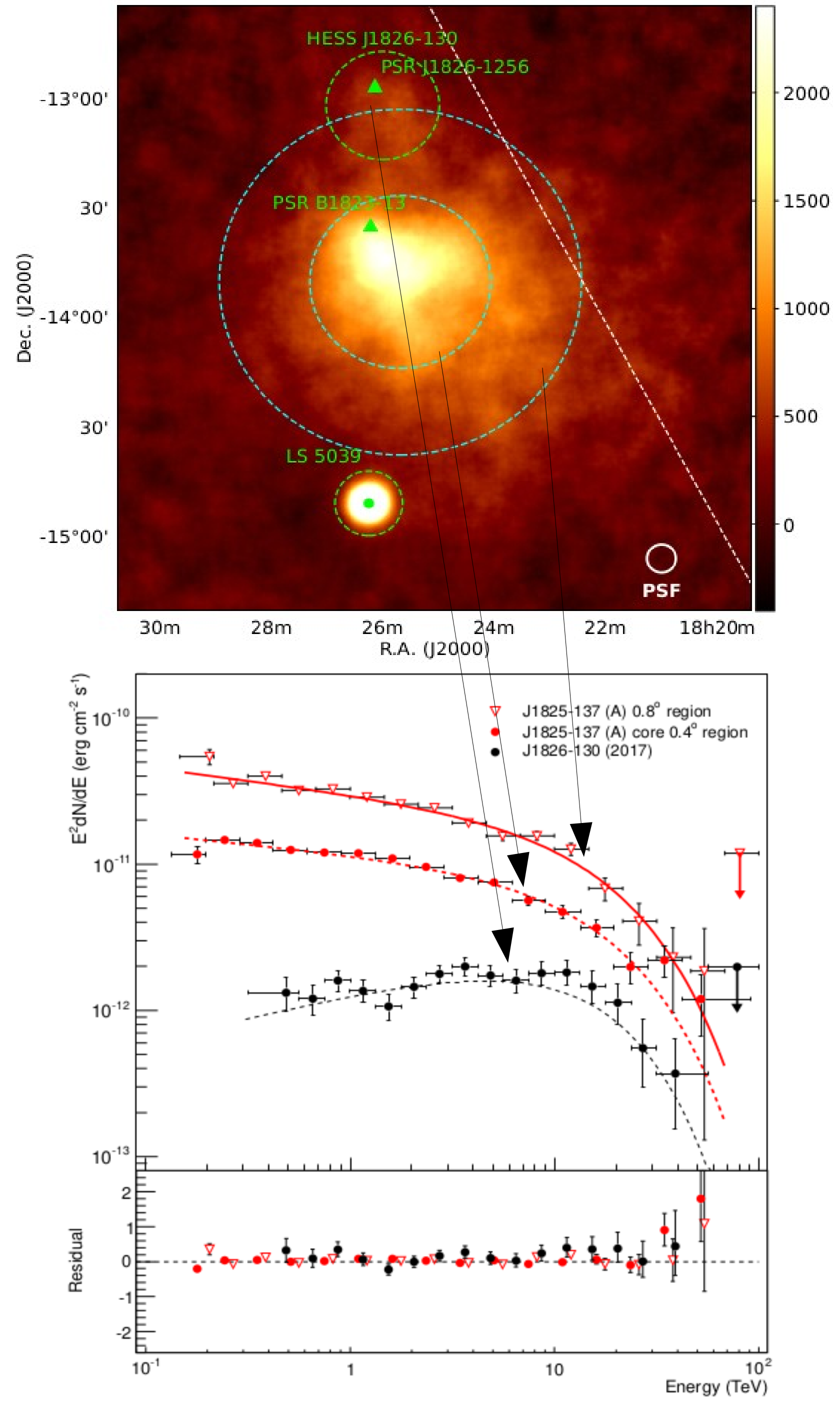

Analysis	Region	ϕ Fit Model	I_0	Γ	Fit Parameters	χ^2/ndf
A	0.4°	$I_0\left(\frac{E}{E_0}\right)^{-\Gamma}$	$6.81 \pm 0.07 \pm 0.2$	$2.28 \pm 0.01 \pm 0.02$	-	141/14
		$I_0\left(\frac{E}{E_0}\right)^{-\Gamma}\exp\left(-\frac{E}{E_c}\right)$	$7.20 \pm 0.09 \pm 0.2$	$2.13 \pm 0.02 \pm 0.03$	$E_c = 19 \pm 3 \pm 0.8$ TeV	21/13
		$I_0\left(\frac{E}{E_0}\right)^{-\Gamma+\beta\log(E/E_0)}$	$7.4 \pm 0.1 \pm 0.1$	$2.26 \pm 0.01 \pm 0.02$	$\beta = 0.078 \pm 0.008 \pm 0.01$	21/13
A	0.8°	$I_0\left(\frac{E}{E_0}\right)^{-\Gamma}$	$17.9 \pm 0.2 \pm 0.4$	$2.33 \pm 0.01 \pm 0.01$	-	134/15
		$I_0\left(\frac{E}{E_0}\right)^{-\Gamma}\exp\left(-\frac{E}{E_c}\right)$	$18.8 \pm 0.2 \pm 0.3$	$2.18 \pm 0.02 \pm 0.02$	$E_c = 19 \pm 3 \pm 2$ TeV	34/14
		$I_0\left(\frac{E}{E_0}\right)^{-\Gamma+\beta\log(E/E_0)}$	$19.3 \pm 0.3 \pm 0.2$	$2.31 \pm 0.01 \pm 0.01$	$\beta = 0.076 \pm 0.009 \pm 0.008$	45/14
B	0.8°	$I_0\left(\frac{E}{E_0}\right)^{-\Gamma}$	$15.0 \pm 0.5 \pm 2$	$2.23 \pm 0.02 \pm 0.04$	-	39/16
		$I_0\left(\frac{E}{E_0}\right)^{-\Gamma}\exp\left(-\frac{E}{E_c}\right)$	$16.1 \pm 0.6 \pm 2.$	$2.06 \pm 0.05 \pm 0.08$	$E_c = 15 \pm 5 \pm 6$ TeV	18/15
		$I_0\left(\frac{E}{E_0}\right)^{-\Gamma+\beta\log(E/E_0)}$	$16.5 \pm 0.6 \pm 2.$	$2.21 \pm 0.03 \pm 0.04$	$\beta = 0.08 \pm 0.02 \pm 0.03$	21/15
H.E.S.S. 2006	0.8°	$I_0\left(\frac{E}{E_0}\right)^{-\Gamma}$	19.8 ± 0.4	2.38 ± 0.02	-	40.4/15
		$I_0\left(\frac{E}{E_0}\right)^{-\Gamma}\exp\left(-\frac{E}{E_c}\right)$	21.0 ± 0.5	2.26 ± 0.03	$E_c = 24.8 \pm 7.2$ TeV	16.9/14
		$I_0\left(\frac{E}{E_0}\right)^{-\Gamma+\beta\log(E/E_0)}$	21.0 ± 0.4	2.29 ± 0.02	$\beta = -0.17 \pm 0.04$	14.5/14

Table 2. Fit parameters for various fits to the nebula spectrum extracted from a symmetric region of 0.8° and 0.4° radius, respectively, with E_0 = 1TeV and I_0 in units of 10^{-12}cm^{-2}s^{-1}TeV^{-1}. In all cases, the first errors quoted are statistical and the second errors are systematic. Curved models are preferred for the results from analysis A, fitted in the energy ranges [0.133,91] TeV in the core region, [0.2, 91] TeV in the 0.8° radius, and for the shorter exposure analysis B in the energy range [0.14, 91] TeV. The fit results from Aharonian et al. (2006b) are also provided for comparison.

Energy dependant morphology

- Very large dataset authorize us to separate dataset in energy bins
- Nebula Vs Energy more and more concentrated around PSR B1823-13
- Effect of propagation + cooling of electrons
- Separation with J1826-130 more clear, confirms that it is two independent sources
- Confirms PSR B1823-130 as a progenitor for the nebula

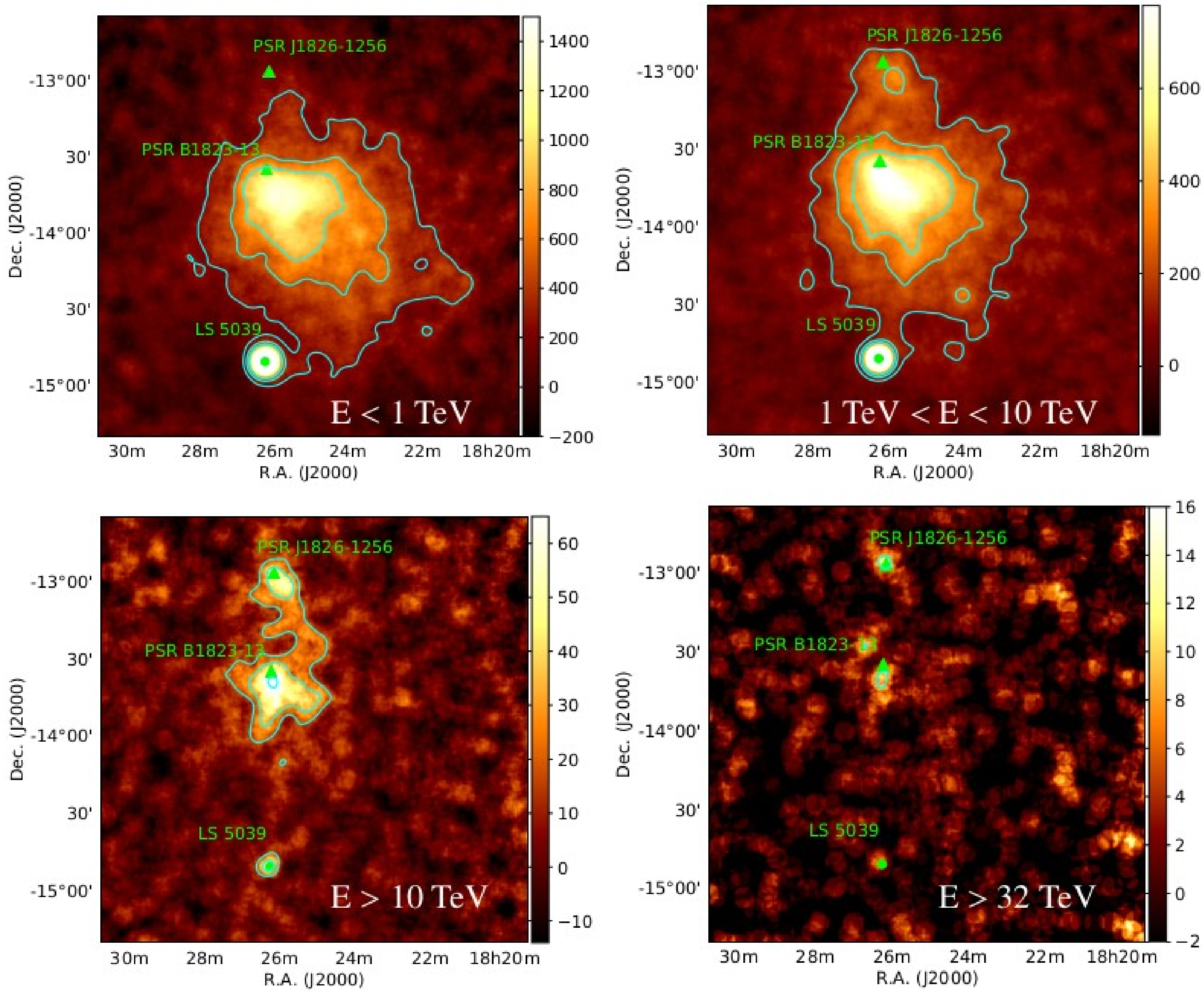

Major-axis and nebula offset determination

- Acceptance corrected counts Vs azimuthal angle
- Major axis of the nebula determined as the distribution mean
- Major Axis 208° +/- 0.6° +/- 10°
- Distribution of counts reconstructed on the direction of the major and minor axis
- Offset on the South and West direction compared to the pulsar
- Maximum of emission found to be offset in the South-West region (0.20°,0.09°)
- Hints of an advection process ?

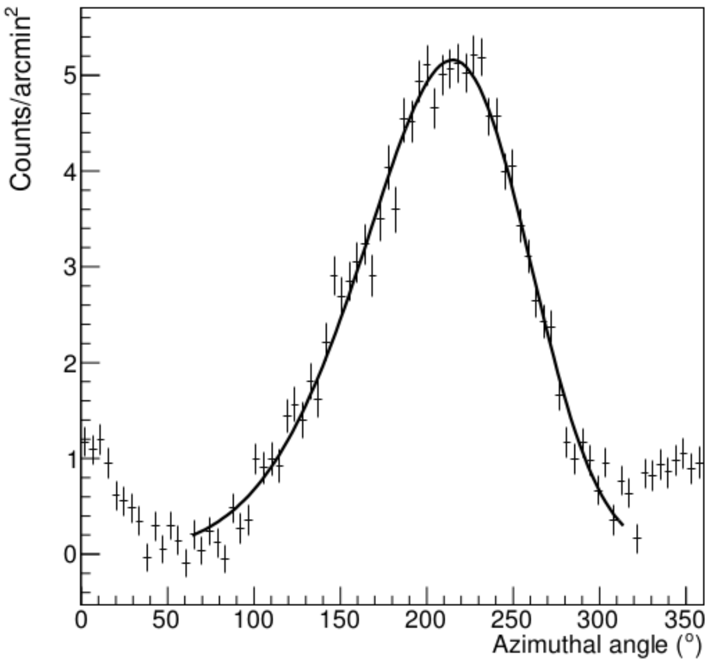

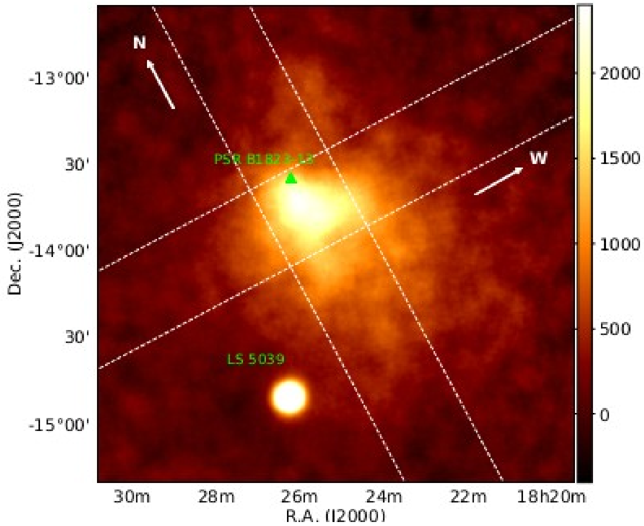

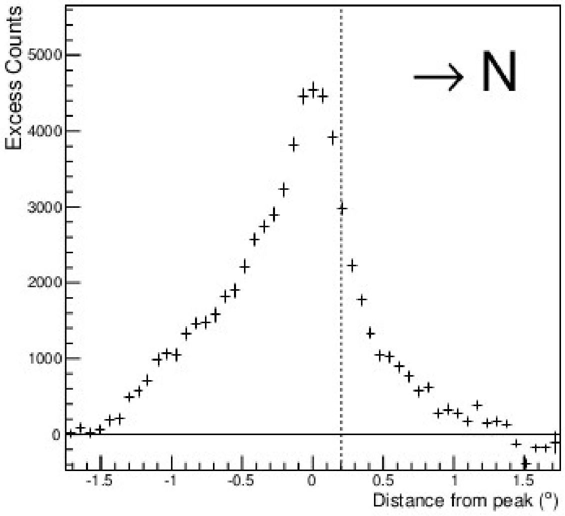

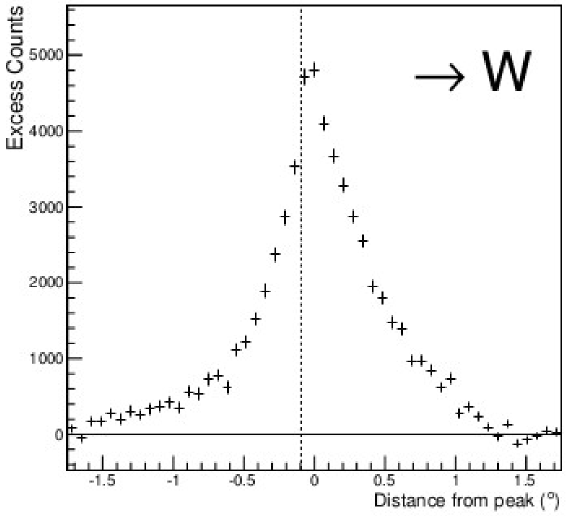

Energy dependent extent measurement

- Extent determined on the the major axis direction (-90°,+90°) versus energy (LS 5039 removed)
- Polynomial function fitted to the corrected counts Vs distance distribution → define the max/exp as the extent

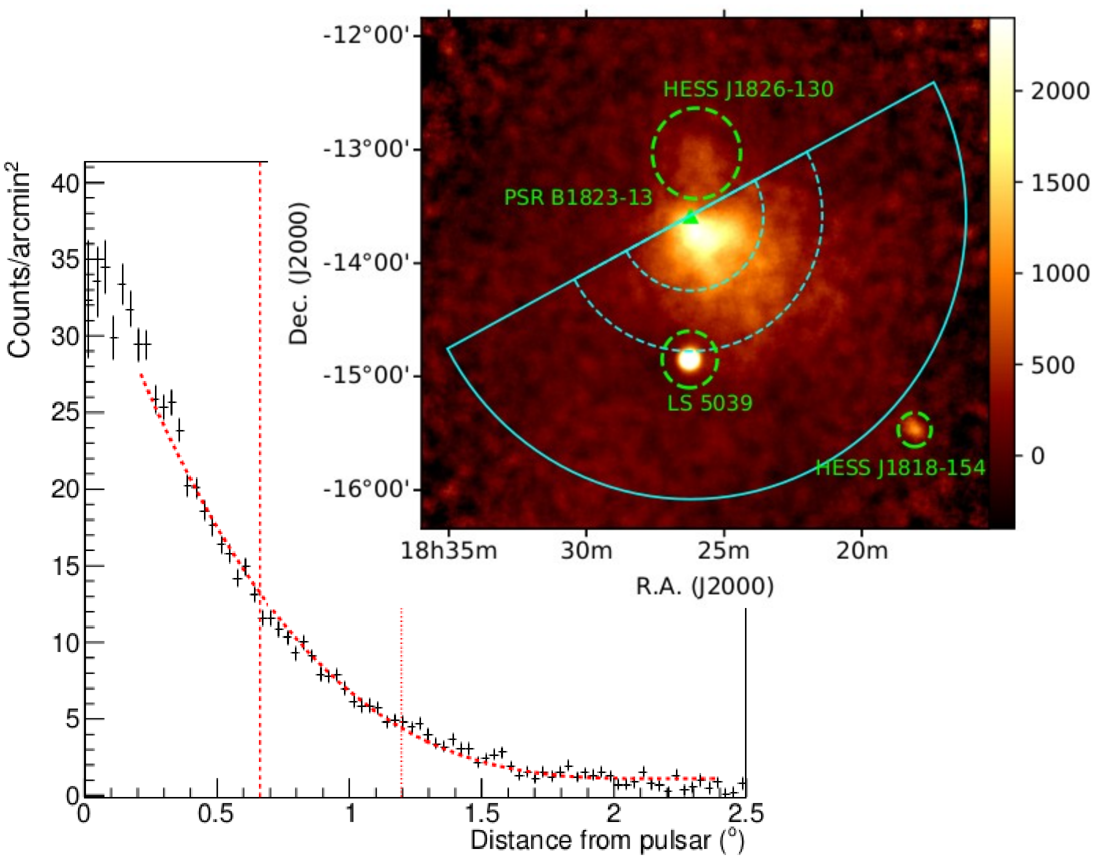

Energy Range	Extent (A)	Extent (B)
< 125 GeV	–	0.37° ± 0.15° ± 0.3°
125 – 250 GeV	–	0.63° ±0.07° ±0.07°
< 250 GeV	0.66° ± 0.04° ± 0.3°	–
250 – 500 GeV	0.76° ± 0.03° ± 0.2°	0.71° ±0.09° ±0.01°
500 GeV –1 TeV	0.72° ±0.02° ±0.05°	0.72° ± 0.05° ± 0.2°
1 – 2 TeV	0.64° ±0.02° ±0.11°	0.62° ± 0.07° ± 0.4°
2 – 4 TeV	0.47° ±0.04° ±0.08°	0.51° ± 0.05° ± 0.1°
4 – 8 TeV	0.38° ±0.04° ±0.13°	0.33° ±0.07° ±0.04°
8 – 16 TeV	0.27° ±0.07° ±0.06°	0.30° ± 0.12° ± 0.3°
> 16 TeV	–	0.22° ± 0.12° ± 0.2°
16 – 32 TeV	0.19° ±0.08° ±0.14°	–
> 32 TeV	0.14° ± 0.1° ± 0.05°	–

Table 3. Extent measurements as a function of energy for analyses A and B, with statistical and systematic errors. The extent is characterised by the radial distance from the pulsar at which the flux reduces to $1/e$ of the peak value in each energy band.

Simple modelling of the energy dependent extension

- Pure diffusion scenario

$$R \propto E_e^{(\delta-1)/2} \qquad 0 \leq \delta \leq 1$$

- Pure advection scenario

$$R \propto E_e^{-\frac{1}{(1+\beta)}} \qquad 0 \leq \beta \leq 2$$

- Inverse Compton scattering

$$E_\gamma \propto E_e^k$$

k = 2 (Thomson)
k = 1 (KN)

Parameter	Value (A)	Value (B)
α	$-0.29 \pm 0.04 \pm 0.05$	$-0.29 \pm 0.06 \pm 0.1$
R_0 (°)	$0.70 \pm 0.02 \pm 0.08$	$0.69 \pm 0.04 \pm 0.2$
δ (T)	$-0.16 \pm 0.15 \pm 0.2$	$-0.17 \pm 0.24 \pm 0.1$
δ (KN)	$0.39 \pm 0.06 \pm 0.2$	$0.4 \pm 0.1 \pm 0.5$
β (T)	$0.7 \pm 0.2 \pm 0.3$	$0.7 \pm 0.3 \pm 0.1$
β (KN)	$2.3 \pm 0.3 \pm 0.8$	$2.3 \pm 0.6 \pm 1$

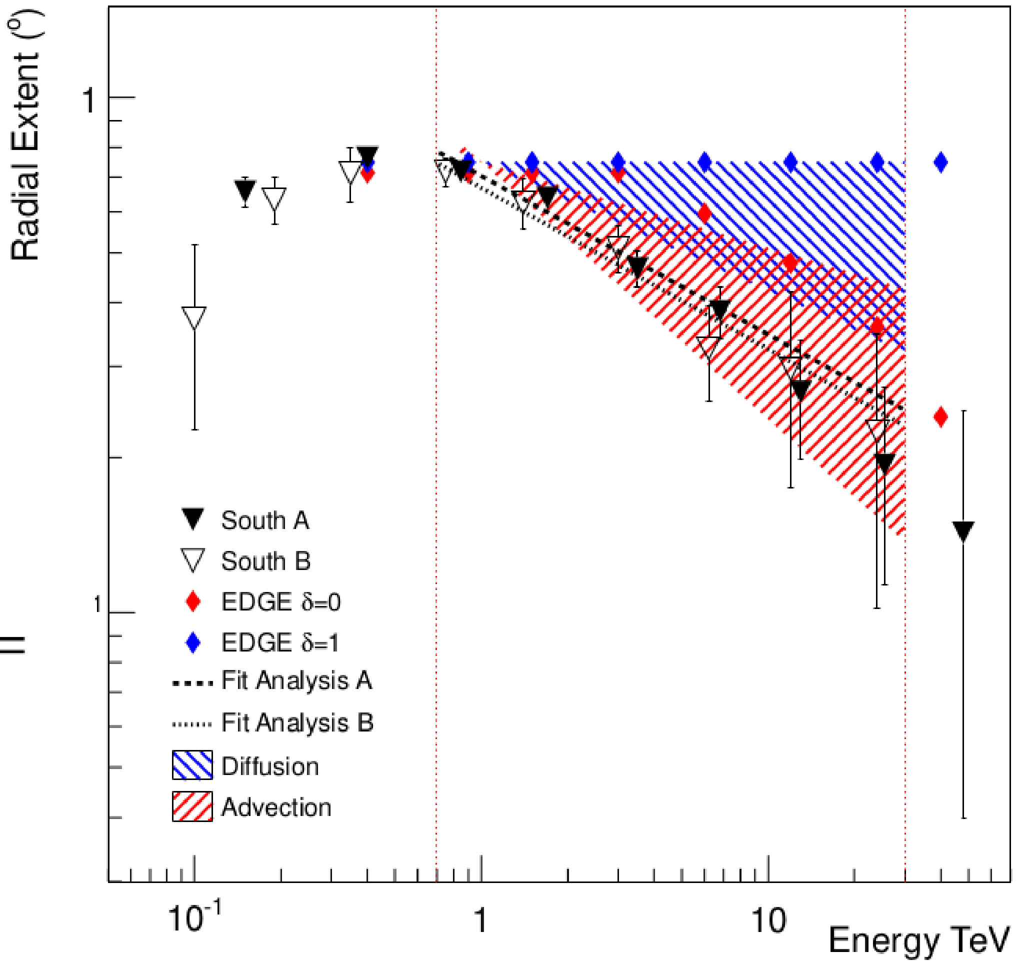

Spectral map

- Important angular size (>>PSF) + important flux give use the opportunity to perform a spectral map of the nebula
- Clear hardening of the spectra for the regions close to the PSR B1823-13

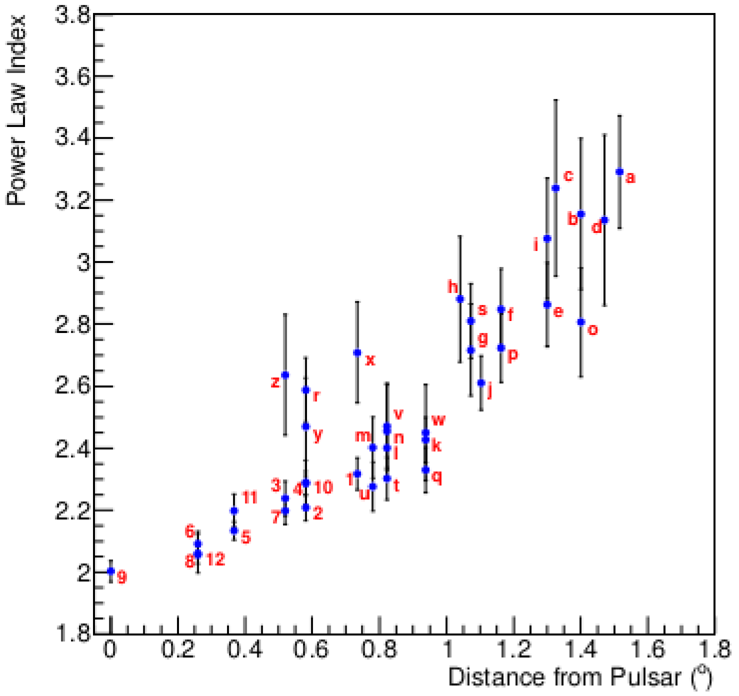

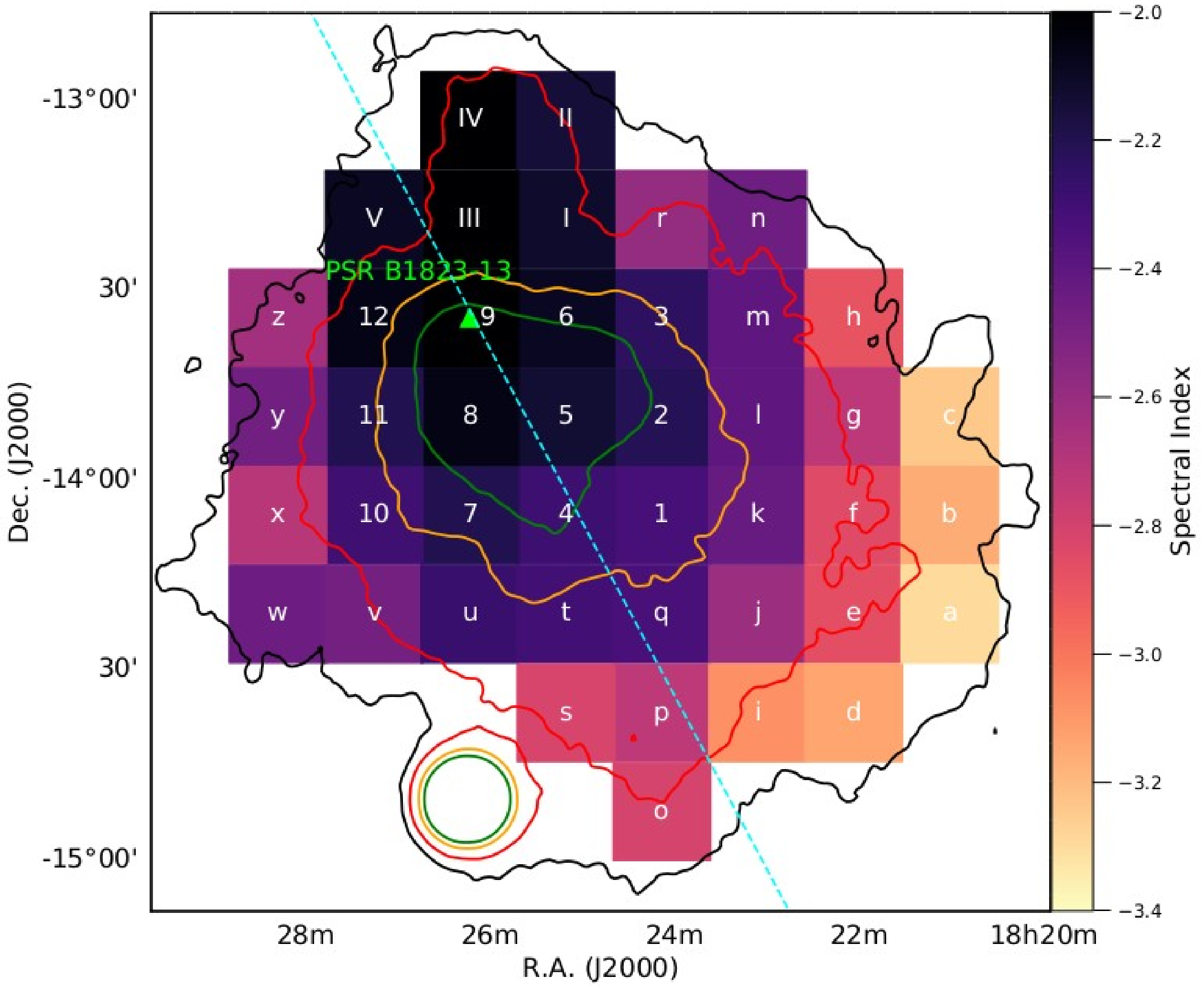

Total nebula spectrum and modelisation of parent population

- Complete nebula flux obtained from combination of the previous spectral map
- Parent population supposed to be leptonic, producing gamma ray through IC
- Using the parameterisation of Popescu et al. for the ISRF and the Naima python package
- Combined HESS and Fermi data well explained by a simple broken power law population

$$\Gamma_1 = 1.4 \pm 0.1$$
$$\Gamma_2 = 3.25 \pm 0.02$$
$$E_b = 0.9 \pm 0.1\,\mathrm{TeV}$$

total energy 5.5×10^{48} erg

- No need for a cut-off in parent population → Thomson to KN transition

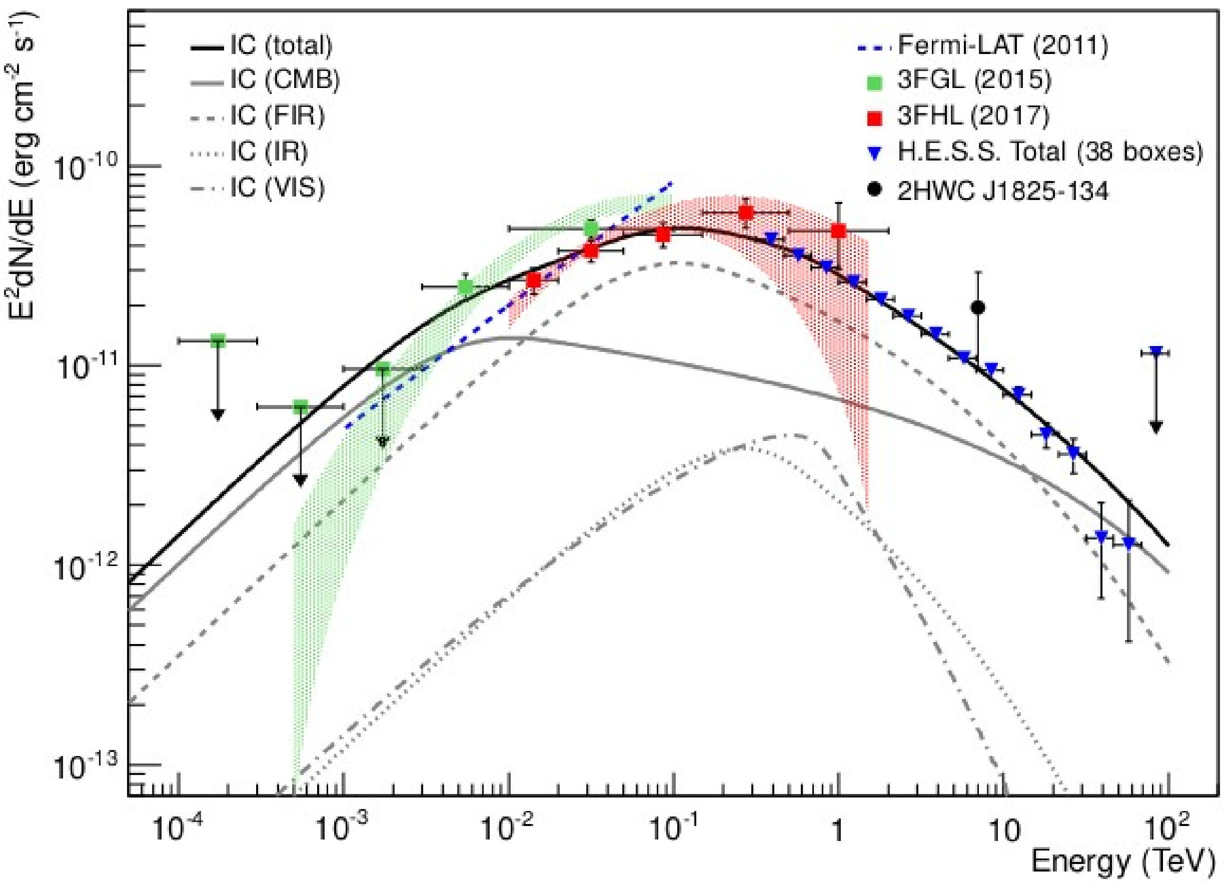

Fermi re-analysis of HESS J1825-137

- Extension at lower energy of the HESS measurement
- Motivated by the larger available dataset compared to the previous Fermi paper (10 yrs) and the understanding of the extent at low energy
- Averaged extension between 1GeV-1TeV (fitted 2D Gaussian) : 1.35° +/- 0.09°
- Bigger extension than HESS results (But not exactly the same method, can't be directly compared)
- Flux Vs Energy compatible with a broken power law

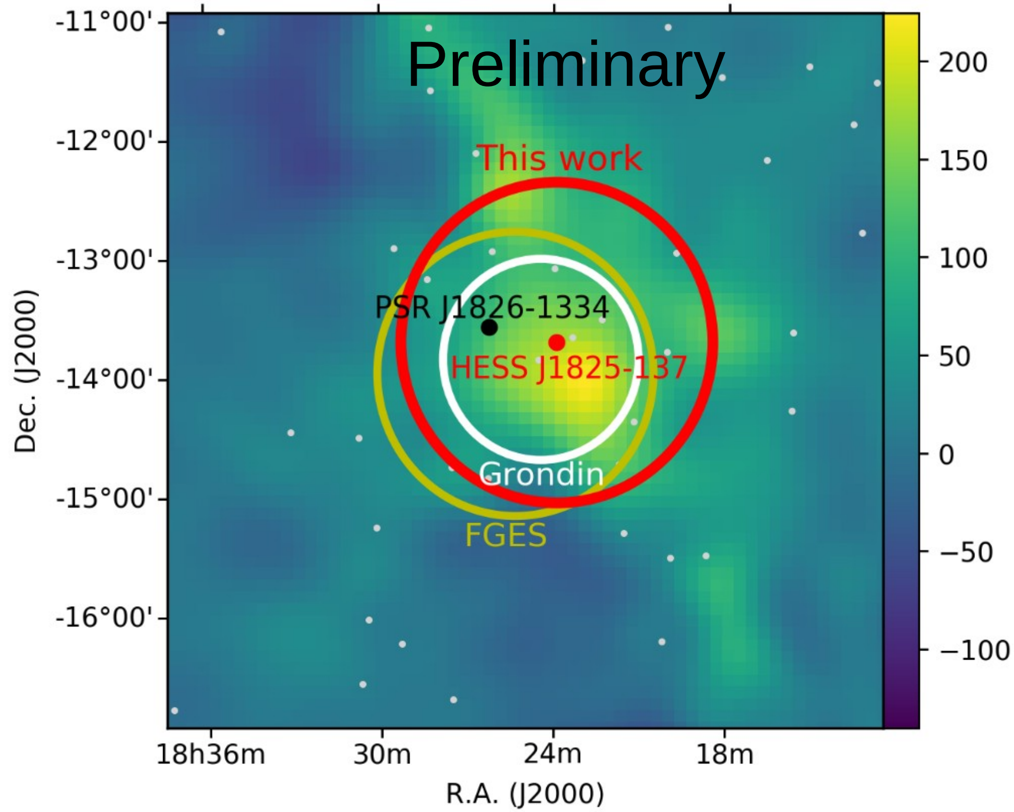

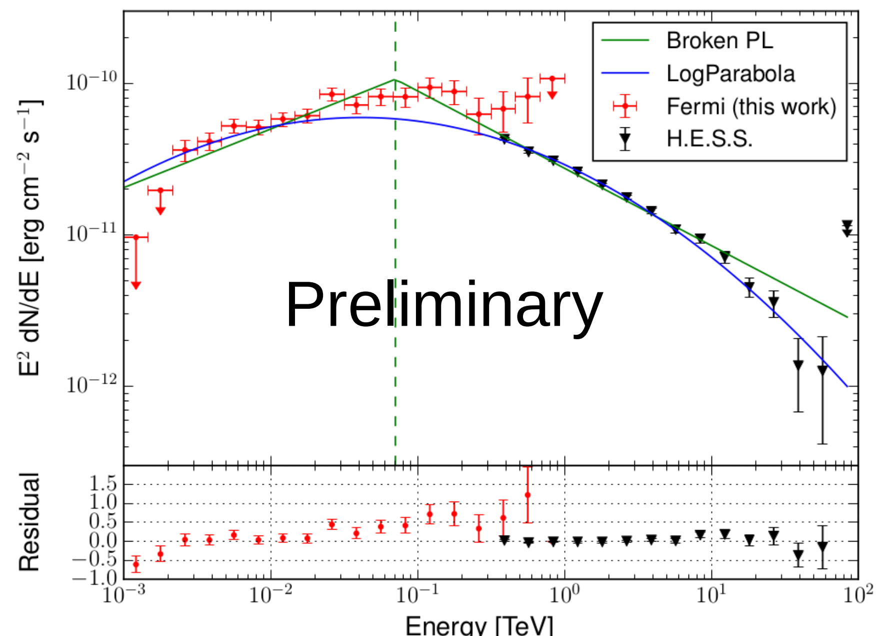

Broken PL

Parameter	*Fermi*	*Fermi* + H.E.S.S.
γ_1	1.50 ± 0.06	1.61 ± 0.03
γ_2	2.04 ± 0.05	2.51 ± 0.01
E_b (GeV)	23.7 ± 4.7	70.6 ± 5.7
N_0 ($\times 10^{-11}$ erg cm−2 s^{-1})	8.26 ± 0.57	10.65 ± 0.43

Energy dependent morphology

- Analysis using 2D Gaussian
- 4 energy bins (3-10, 10-30, 10-100, 100-1000 GeV)
- Same behavior than HESS is observed

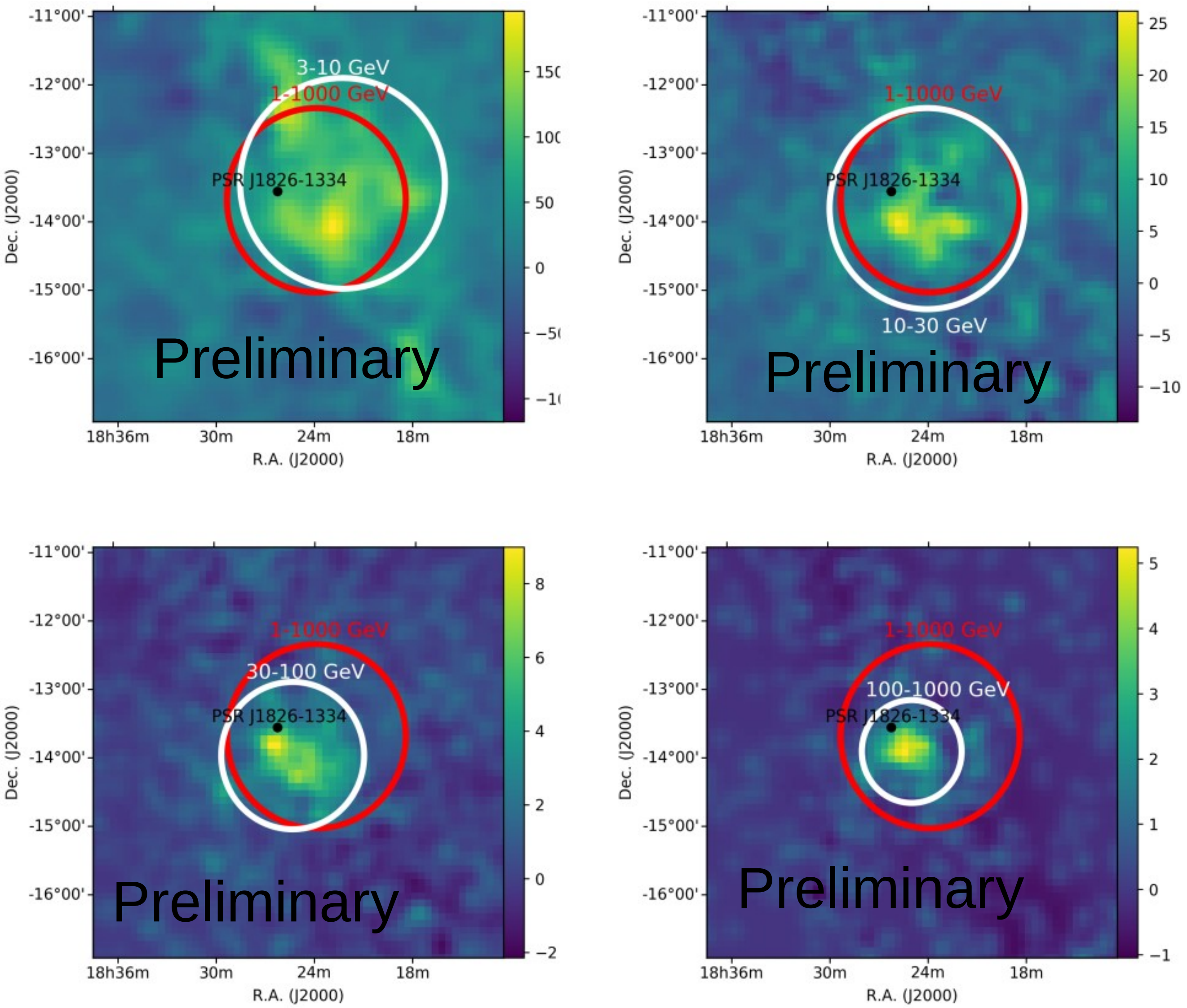

Combined fit extent Fermi-LAT + HESS

- Source extension versus energy using 2D Gaussian (blue points) and a HESS-like method (black points)
- Power law fit on the full range and advection and propagation index derived

Parameter	Value
α	-0.192 ± 0.007
R_0	$0.62^\circ \pm 0.02$
δ	0.23 ± 0.03
β	1.61 ± 0.09

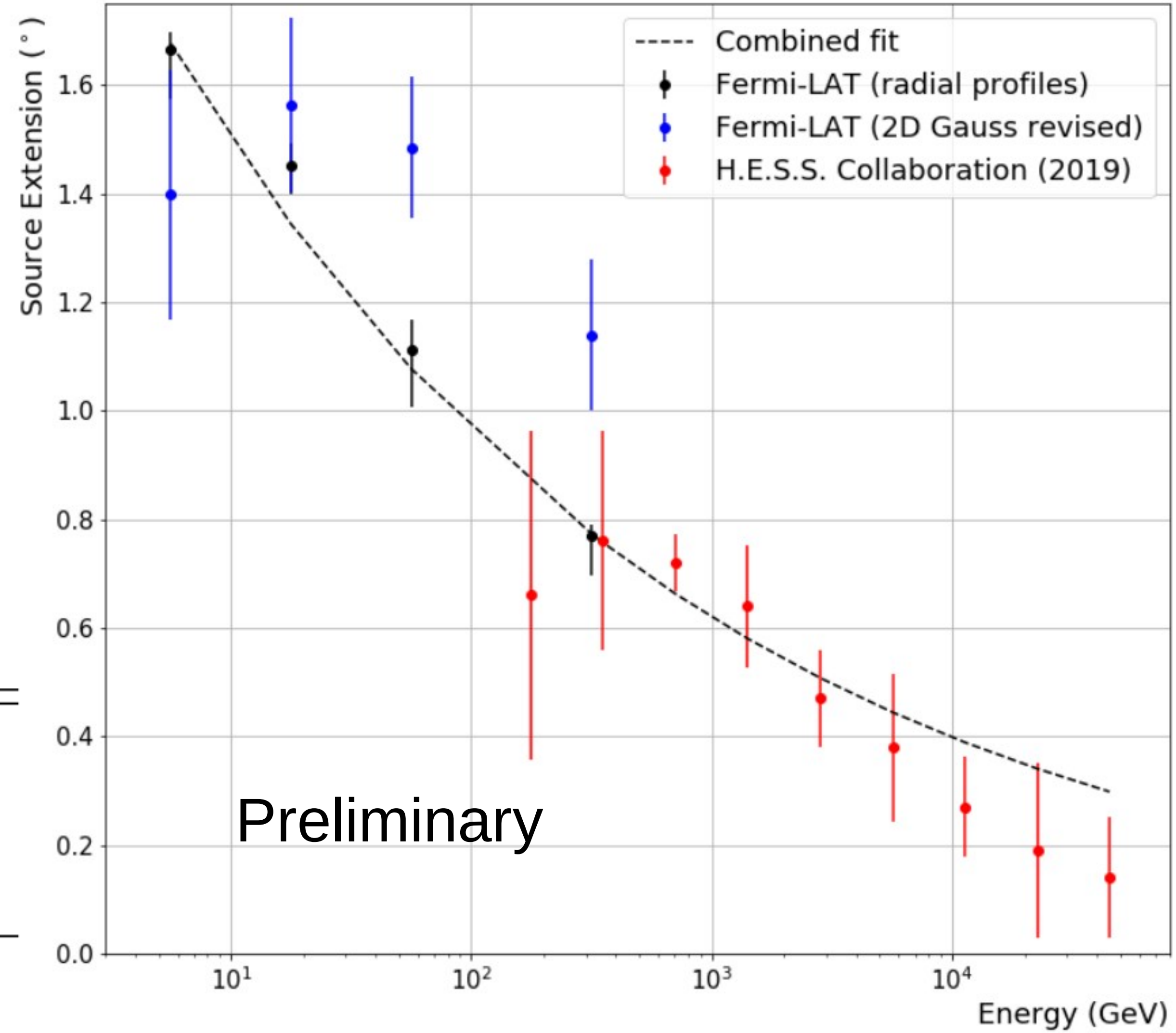

Conclusion and outlook

- HESS J1825-137 is a source with a very rich dataset and multi-wavelength context (X-ray, Fermi, HESS, HAWC ?)
- Thanks to its large extent and the efficient IC boost by FIR, we tested various propagation model (advection, diffusion)
- Lots of data usefull for a deeper modelling was extracted from HESS data (Flux map, Total flux, geometry) and are available
- This is the most extended PWN (up to 100 pc), this is a chance to have a better general understanding of particle propagation inside PWN

Cooling typical time

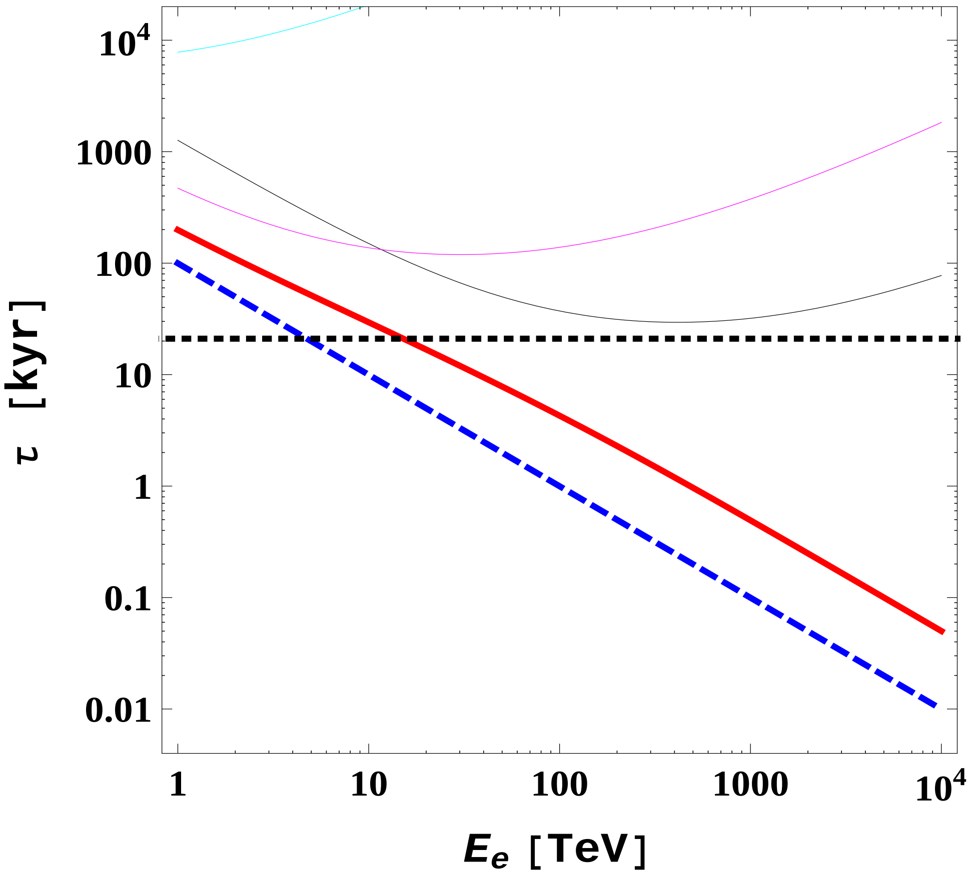

ISRF model (4.8 kpc gal center)

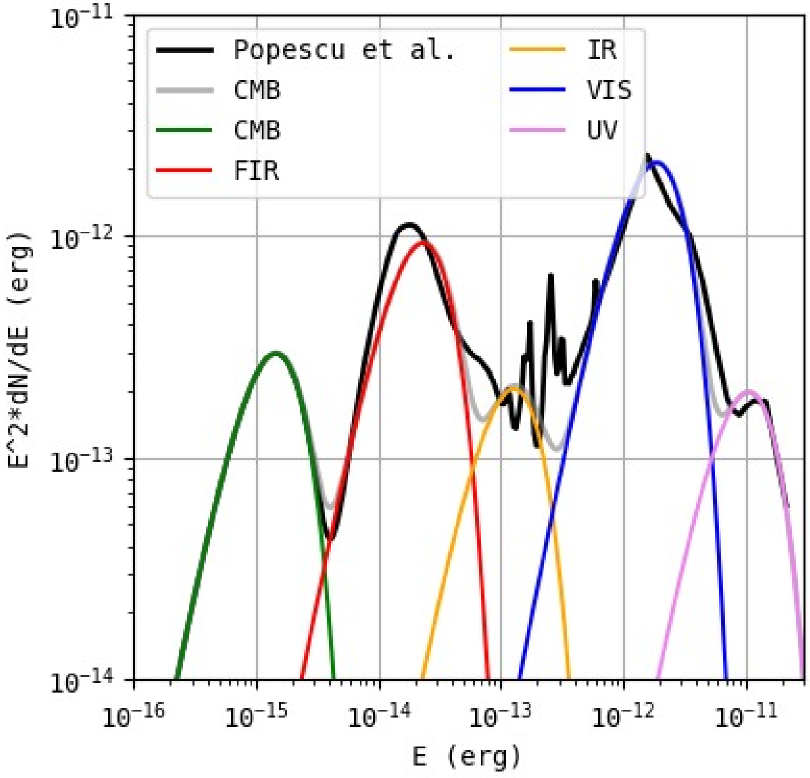

The radiation field model of Popescu et al. (2017) for the Galactic location of HESS J1825-137 can be approximated by four black-body components; the cosmic microwave background (CMB) with a temperature T of 2.7 K and an energy density ω of 0.25 eVcm^{-3}; the far-infrared (FIR, dust, $T \sim 40$ K, $\omega \sim 1$ eVcm^{-3}); near-infrared (NIR, T $\sim$ 500 K, $\omega \sim 0.4$ eVcm^{-3}), and visible light (VIS, $T \sim 3500$ K, $\omega \sim 1.9$ eVcm^{-3}). IC scat-